Solid-State NMR Study of Hydrated Intercalation Compounds of Molybdenum Disulfide

V. Alexiev,[‡] H. Meyer zu Altenschildesche,[†] R. Prins,[†] and Th. Weber*[,†]

Laboratory for Technical Chemistry, Swiss Federal Institute of Technology (ETH), 8092 Zurich, Switzerland, and Institute of Catalysis, Bulgarian Academy of Sciences, 1113 Sofia, Bulgaria

Received December 11, 1998. Revised Manuscript Received April 19, 1999

Solid-state NMR has been used to study the local coordination environments of the protons and alkali metal cations in hydrated alkali metal intercalation compounds of MoS_2, $A_x(H_2O)_yMoS_2$ (A = Li, Na, K, Cs). The dynamic behavior of the water molecules, which are coordinated to the intercalated A^+ cations, is consistent with an ordered quasi two-dimensional translational motion at room temperature. In $Li_x(H_2O)_yMoS_2$, the hydrated Li^+ cations occupy two distinct sites in the van der Waals gap that are connected by dynamic processes. Partially random motions of the H_2O molecules are activated at room temperature.

Introduction

Intercalation compounds of the groups 4−6 transition metal dichalcogenides (MX_2) have attracted much attention in recent years. These compounds are highly anisotropic and are often referred to as *two-dimensional solids*. The presence of a nonstoichiometric number of molecules and ionic species between the layers of MX_2 has a profound influence on the structure and on the electronic properties of the host lattice, on order−disorder phenomena, on the magnetic properties, and on superconductivity.[1,2] Intercalation of alkali metal cations between the layers of molybdenum disulfide (MoS_2) provides a relatively easy way to tune the electron occupation of the d-bands. These compounds provide useful solid-state models for alkali metal-promoted MoS_2-type phases, recently recognized to be alternative catalysts in the *water gas shift* reaction ($CO + H_2O \rightarrow CO_2 + H_2$). Whereas A_zMoS_2 intercalation compounds (A = Li, Na, K, Cs; $z \leq 1$) are very useful for learning more about the electronic structure of the alkali metal-promoted MoS_2-type phases, the activation mechanism of H_2O molecules during water gas shift catalysis can be studied by using hydrated alkali metal intercalates of MoS_2 ($A_x(H_2O)_yMoS_2$) as model compounds.

Hydrated alkali metal intercalation compounds of MoS_2 consist of MoS_2 slabs with the hydrated A^+ cations in the space between the slabs (i.e., in the van der Waals gap). Depending on the hydration enthalpy of the respective alkali cation, single layers or bilayers of water molecules form around the A^+ cation.[3−8] The hydrated intercalates are usually obtained from the unhydrated compounds (A_zMoS_2) by reaction with water.[9−13]

Upon intercalation, the local coordination geometry of the Mo centers of the host lattice changes from trigonal prismatic (as in the thermodynamically favored 2H-MoS_2) to distorted octahedral (as in the metastable 1T-MoS_2). This 2H → 1T phase transition is accompanied by considerable changes in the band structure, an increased electron density on the sulfur atoms of the MoS_2 lattice, and the formation of different types of superstructures.[14,15] In contrast to 2H-MoS_2, the electronic properties of the host lattices of 2H-NbS_2 and 1T-TiS_2 are preserved during intercalation. The only change is an increased d-band filling and a reduction in the density of states at the Fermi level.[16]

The static structure and dynamic behavior of intercalation compounds of groups 4 and 5 transition metal sulfides, MS_2 (M = Ti, Zr, V, Nb, Ta), have been studied in detail.[3−8,16] The structural properties and the observed dynamic behavior of the intercalated species were explained in terms of a quasi two-dimensional motion of water molecules. Depending on the extent of hydration, the water molecules can be found in two different orientations. While the H−H vectors of the H_2O molecules are parallel to the crystallographic *c*-axis of the host lattice in the monolayered compounds

---

* Address correspondence to Dr. Thomas Weber, Laboratory for Technical Chemistry, ETH-Zentrum, Universitätstr. 6, 8092 Zurich, Switzerland. Phone: +41 1 632 3043. Fax: +41 1 632 1162. E-mail: thomas.weber@tech.chem.ethz.ch.

[†] Swiss Federal Institute of Technology.

[‡] Bulgarian Academy of Sciences.

(1) Friend, R. H.; Yoffe, A. D. *Adv. Phys.* **1987,** *36,* 2.

(2) Schöllhorn, R. In *Progress in Intercalation Research*; Müller-Warmuth, W., Schöllhorn, R., Eds.; Kluwer: Dordrecht, 1994; p 1.

(3) Röder, U.; Müller-Warmuth, W.; Schöllhorn, R. *J. Chem. Phys.* **1979**, *70*, 2864.

(4) Röder, U.; Müller-Warmuth, W.; Schöllhorn, R. *J. Chem. Phys.* **1981**, *75*, 412.

(5) Röder, U.; Müller-Warmuth, W.; Spiess, H. W.; Schöllhorn, R. *J. Chem. Phys.* **1982**, *77*, 4627.

(6) Kanzaki, Y.; Watanabe, N.; Maeda, K.; Matsumoto, O. *J. J. Phys. Chem.* **1987**, *91*, 2727.

(7) Halsted, T.; Schmidt, C.; Spiess, H. W.; Schöllhorn, R.; Müller-Warmuth, W.; Möller, H. *J. Phys. Chem.* **1988**, *92*, 7167.

(8) Lobert, M.; Müller-Warmuth, W.; Paulus, W.; Schöllhorn, R. *Colloids Surf., A* **1993**, *72*, 345.

(9) Schöllhorn, R.; Meyer, H. *Mater. Res. Bull.* **1974**, *9*, 1237.

(10) Lerf, A.; Schöllhorn, R. *Inorg. Chem.* **1977**, *16*, 2950.

(11) Schöllhorn, R.; Kumpers, M.; Plorin, D. *J. Less-Common Met.* **1978**, *58*, 55.

(12) Py, M. A.; Haering, R. R. *Can. J. Phys.* **1983**, *61*, 79.

(13) Mulhern, P. J. *Can. J. Phys.* **1989**, *67*, 1049.

(14) Wypych, F.; Weber, Th.; Prins, R. *Surf. Sci.* **1997**, *32*, L474.

(15) Wypych, F.; Weber, Th.; Prins, R. *Chem. Mater.* **1998**, *10*, 723.

(16) Lobert, M.; Müller-Warmuth; W.; Schöllhorn, R. *Ber. Bunsen-Ges. Phys. Chem.* **1992**, *96*, 1564.

10.1021/cm980780z CCC: $18.00

(Figure 1a), the H−H vectors are distributed in cones that form an angle of approximately 45° with the crystallographic *c*-axis in the bilayered phases (Figure 1b). Below a certain temperature T^*, in the 140−350 K temperature range, wide-line NMR spectra, characteristic of rigid water molecules, and both intra- and intermolecular dipole−dipole couplings are observed.[3−5] At temperatures above T^*, wide-line ^1H NMR spectra with typical Pake shapes are well resolved, indicating that dipolar coupling arises only from intramolecular interaction within the water molecule. An ordered, sufficiently rapid translational motion of the H_2O molecules is postulated which averages intermolecular dipole−dipole interactions and changes the relative positions of the water molecules. The electrostatic anion−dipole interaction of the delocalized negative charges of the sulfur layers with the positively polarized hydrogen atoms of H_2O hinders rotation around the C_2 axes in the range of ordered mobility, while the translational motion retains the orientation of the protons relative to the layers. At elevated temperatures (>300 K), the Pake spectrum broadens and a narrow component appears in the center, typical of rapid proton exchange and a partially random motion of the water molecules. In the bilayered hydrates, the barrier for the C_2 axis spinning is lower, and this rotation is observed along with the translational motion.

The present paper reports an investigation of the $A_x(H_2O)_yMoS_2$ (A = Li, Na, K, Cs; $x = 0.3$) compounds by means of ^1H, ^{27}Na, ^7Li, and ^{133}Cs NMR, powder X-ray diffraction (XRD), and magnetic susceptibility measurements at room temperature. The data presented yield information about the structures of these compounds and the dynamic behavior of the guest species.

Experimental Section

Powder XRD patterns were measured on a TUR M62 diffractometer (0.178 nm Co Kα radiation) equipped with a computer-controlled HZG-4 goniometer. Magnetic susceptibility measurements were performed on a Faraday-type balance at room temperature (293 K).

K_xMoS_2 and Na_xMoS_2 were prepared from A_2MoO_4 (A = Na, K) by sulfidation ($A_2MoO_4 + 4H_2S \rightarrow A_2MoS_4 + 4H_2O$), subsequent reduction ($2A_2MoS_4 + 3H_2 \rightarrow 2A_zMoS_2 + 2yA^0 + A_2S + 3H_2S$, $y < 1$, $z = 1 - y$), and hydration ($A_zMoS_2 + (n + y)H_2O \rightarrow A_x(H_2O)_yMoS_2 + (n/2)H_2 + nAOH$, $x = z - n$). Li_xMoS_2 was prepared by treating 2H-MoS_2 (Fluka) with *n*-buthyllithium for several days, followed by exfoliation in H_2O and restacking. A detailed description of the preparation of $A_x(H_2O)_yMoS_2$ (A = Li, Na, K) can be found in the literature.[14,17−19] $Cs_x(H_2O)_yMoS_2$ was obtained from the corresponding sodium compound by ion exchange with CsCl.

All NMR measurements were performed at room temperature on a Bruker AMX400 instrument ($B_0 = 9.4$ T, wide-bore magnet) using a double-tuned magic-angle-spinning (MAS) probe. The samples were poured into zirconia rotors (outer diameter, 4 mm) and sealed with Kel-F caps. ^1H solid-echo spectra of the static samples were obtained using a $(\pi/2)_x-\tau-(\pi/2)_y-\tau$ pulse sequence with a radio frequency field strength of ~50 kHz. For all other experiments, single-pulse excitation followed by data acquisition was used. ^1H spectra were referenced externally to tetramethylsilane (TMS), while the ^7Li, ^{23}Na, and ^{133}Cs spectra were referenced to 1 M aqueous solutions of $LiNO_3$, NaCl, and CsCl, respectively. Short excitation pulses, i.e., tip angles < $\pi/12$, were used to obtain the spectra of the quadrupolar nuclei ^7Li, ^{23}Na, and ^{133}Cs in order to ensure quantitative reliability of the data. MAS spinning speeds were in the range of 8−12 kHz and are indicated in the figure captions. In contrast to previous studies,[3−8,16] no magnetic field-induced preferred orientation of crystallites was observed for the samples studied.

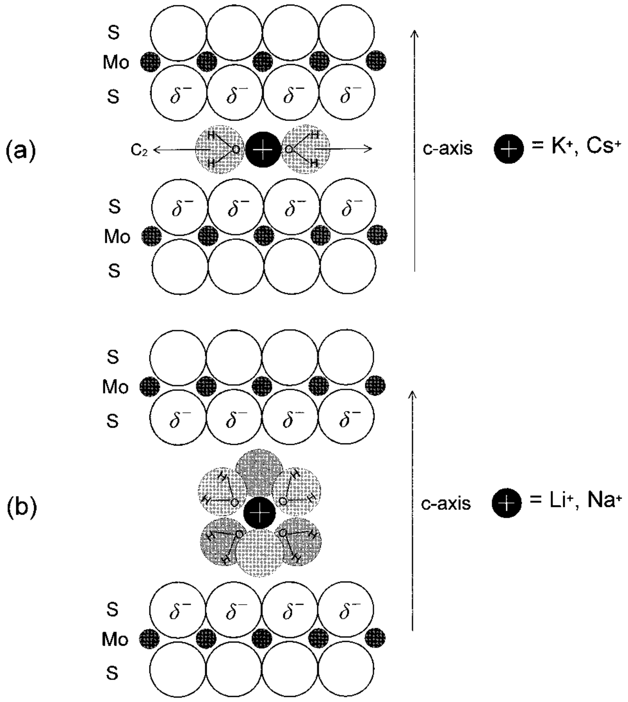

Figure 1. Schematic presentation of the arrangement of water molecules in the monolayered (a) and bilayered (b) $A_x(H_2O)_yMoS_2$ intercalation compounds.

The static ^1H NMR spectra were analyzed with respect to chemical shift anisotropy and proton−proton dipolar interactions using the program SOLIDS.[20] The conventions for the elements of the chemical shift tensor, the dipolar coupling tensor, and the angles describing their relative orientation follow ref 20. Appropriate line broadenings were used to get optimum fits.

Results

Figure 2 shows the XRD patterns of the $A_x(H_2O)_yMoS_2$ intercalation compounds. The positions and intensities of the reflections are in agreement with previously reported data.[9,11−13] In contrast to that of the Na, K, and Cs derivatives, the crystallinity of the Li compound is poor. This property can be correlated directly with the preparation procedure. $Li_x(H_2O)_yMoS_2$ was not obtained from high-temperature synthesis but by the reaction of 2H-MoS_2 with *n*-buthyllithium at room temperature, followed by hydration with water. During this treatment, the crystalline 2H-MoS_2 becomes nearly amorphous. Analysis of the XRD patterns (Figure 2) shows that the interlayer height is 310−320 pm in $Cs_x(H_2O)_yMoS_2$ and $K_x(H_2O)_yMoS_2$ and 560−590 pm in $Li_x(H_2O)_yMoS_2$ and $Na_x(H_2O)_yMoS_2$.[9,11] These findings are consistent with the different degree of hydration in these materials. Whereas a single layer of H_2O molecules

---

(17) Dines, M. B. *Mater. Res. Bull.* **1975**, *10*, 287.

(18) Joensen, P.; Frindt, R. F.; Morrison, S. R. *Mater. Res. Bull.* **1986**, *21*, 457.

(19) Wypych, F.; Schöllhorn, R. *J. Chem. Soc., Chem. Commun.* **1992**, 1386.

(20) Eichele, K.; Wasylishen, R. E. *J. Magn. Reson. A* **1994**, *106*, 46.

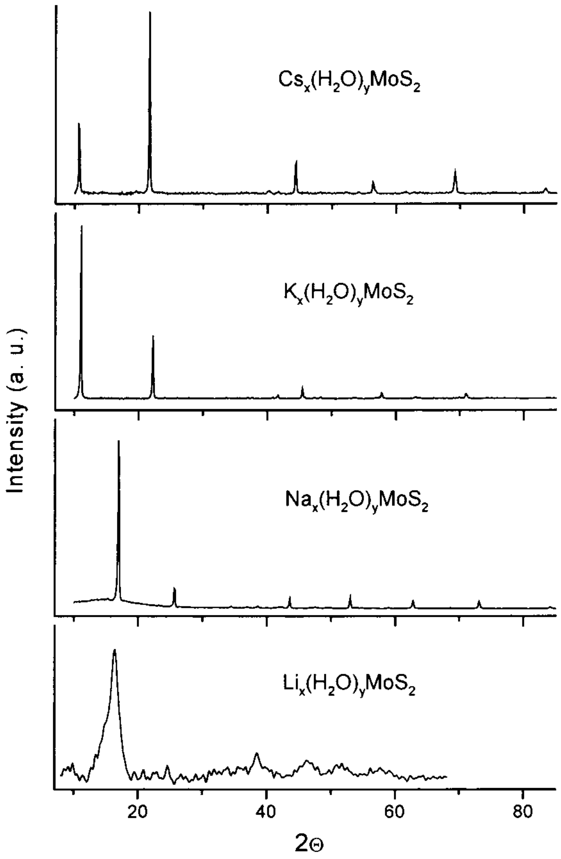

Figure 2. X-ray powder diffraction patterns of the $A_x(H_2O)_yMoS_2$ intercalation compounds.

surrounds the intercalated Cs^+ and K^+ cations, the fully hydrated Li and Na phases contain bilayers of H_2O.

^{1}H NMR Spectra. The static ^{1}H NMR spectra of $Cs_x(H_2O)_yMoS_2$ and $K_x(H_2O)_yMoS_2$ display a Pake line shape superimposed by a Gaussian peak at the center (Figure 3a,b). The ^{1}H MAS spectra of both compounds (Figure 3e,f) show only two differences: the values of the chemical shift of H_2O molecules coordinated to the A^+ cations (Cs, 4.5 ppm; K, 3.7 ppm; see Table 1) and the intensity of the peak due to adsorbed water observed as a shoulder at 2.7 ppm. As can be seen in the static NMR spectra, only intramolecular dipole interactions between the two protons in a water molecule are operative, and the effective proton dipole splitting of the Cs intercalation compound is smaller than that observed for $K_x(H_2O)_yMoS_2$. The chemical shift anisotropy $\Delta\sigma$ is −2.7 ppm with axial symmetry in the case of $Cs_x(H_2O)_yMoS_2$, while no anisotropy was found for $K_x(H_2O)_yMoS_2$. Table 1 summarizes all the values measured from the ^{1}H MAS NMR experiments and the parameters used in the simulations of the static spectra. As a representative example, the simulation of the static powder spectrum for $K_x(H_2O)_yMoS_2$ is shown in Figure 4.

In contrast, the double-layered intercalates $Na_x(H_2O)_yMoS_2$ and $Li_x(H_2O)_yMoS_2$ display more complicated ^{1}H NMR spectra (Figure 3c,d). The wide-line ^{1}H NMR spectrum of $Na_x(H_2O)_yMoS_2$ (Figure 3c) consists of a fairly weak Pake doublet and an intense central peak with a smaller shoulder. Evacuation of the sample for 1 h at a pressure of 1×10^{-3} Pa reduced the intensity of the central line (at 6.9 ppm) by 20% relative to the Pake doublet and resulted in an increased resolution of the shoulder (−7 ppm). Two narrow peaks and a broad feature were identified in the corresponding ^{1}H MAS spectrum of this compound (Figure 3g). Their positions relative to TMS are given in Table 1, together with the parameters that produce the best simulation of the Pake part of the static spectrum. The essential result of the simulation is the greater chemical shift anisotropy and the larger effective dipolar coupling constant of this compound compared to the K and Cs intercalates. However, the narrow peak in the center represents a large portion of the protons that do not exhibit strong dipolar interactions.

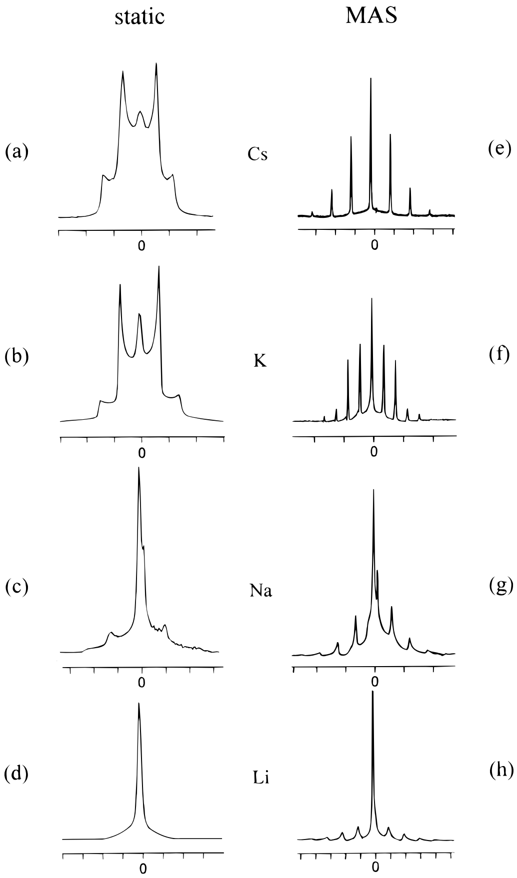

Figure 3. Solid-state ^{1}H NMR spectra (left column, static; right column, MAS) of the $A_x(H_2O)_yMoS_2$ intercalation compounds. The MAS spectra were obtained at the following spinning speeds: 10 (Cs), 8 (K), 12 (Na), and 10 kHz (Li).

Table 1. Measured and Simulated ^{1}H NMR Parameters and Magnetic Properties for $A_x(H_2O)_yMoS_2$

	$\sigma_0{}^a$	$\sigma_{11}{}^b$	$\sigma_{22}{}^b$	$\sigma_{33}{}^b$	$\Delta\sigma^b$	$R_{eff}{}^c$	$\mu_{eff}{}^d$
Li $_x(H_2O)_yMoS_2$	4.3(*), −0.2(sh)						1.01
$Na_x(H_2O)_yMoS_2$	7(sh), 6.9(*), −7.2	9	7	−2.0	−10.0	24 200	0.56
$K_x(H_2O)_yMoS_2$	3.7(*), 2.7(sh)	3.9	3.9	3.9	0.0	20 490	0.62
Cs $_x(H_2O)_yMoS_2$	4.5(*), 2.7(vw, sh)	8.3	8.3	5.6	−2.7	17 750	0.59

[a] MAS isotropic values in ppm. *, main peak; sh, shoulder; vw, very weak. [b] Values of the chemical shift tensor σ_{xx} and the anisotropy of the chemical shift $\Delta\sigma$ in ppm, obtained by simulating the Pake pattern part of the spectra. [c] Effective dipolar couplings in hertz, obtained by simulating the Pake pattern part of the spectra.[20] [d] μ_{eff} in Bohr magnetons.

The static^{1}H NMR spectrum of $Li_x(H_2O)_yMoS_2$ (Figure 3d) is different from the spectra described thus far. It

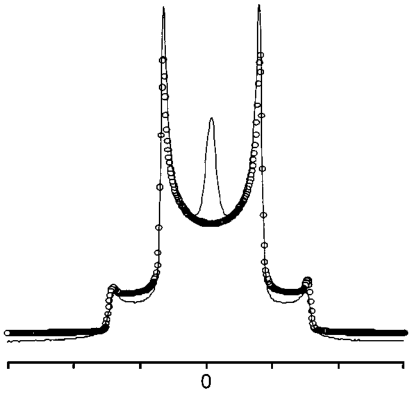

Figure 4. Experimental (—) and simulated (○) ^1H static spectra of a polycrystalline sample of $K_x(H_2O)_yMoS_2$.

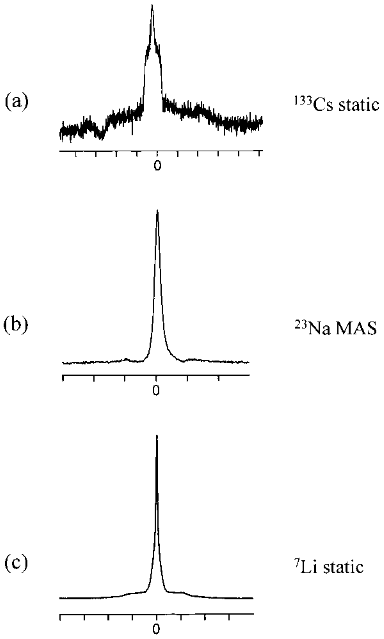

Figure 5. ^{133}Cs static (a), ^{23}Na MAS (b), and ^7Li static (c) NMR spectra of $Cs_x(H_2O)_yMoS_2$, $Na_x(H_2O)_yMoS_2$, and $Li_x(H_2O)_yMoS_2$.

consists of only one intense peak at 4.3 ppm with weak, unresolved wings of low intensity. A single peak with a shoulder is observed in the ^1H MAS spectrum of this sample (Figure 3h). Since the static spectrum is featureless, no simulation of the NMR static powder spectrum was attempted for this sample.

^{7}Li, ^{23}Na, and ^{133}Cs NMR Spectra. To gain more information about the residence site of the alkali cation in the van der Waals gap, ^7Li, ^{23}Na, and ^{133}Cs NMR measurements of $Li_x(H_2O)_yMoS_2$, $Na_x(H_2O)_yMoS_2$, and $Cs_x(H_2O)_yMoS_2$ were performed. Figure 5 displays the ^7Li and ^{133}Cs static spectra as well as the ^{23}Na MAS spectrum of the corresponding hydrated intercalates. The parameters obtained from the NMR experiments are listed in Table 2. The intrinsic anisotropy of the host lattice is clearly manifested in the ^{133}Cs NMR spectra and shows up as a nonaxially symmetric CSA tensor (the singularities of the pattern are found at 131, 175, and 213 ppm). The distorted baseline of the static spectrum clearly points toward the presence of a first-order quadrupole interaction. The ^{133}Cs MAS NMR spectrum of $Cs_x(H_2O)_yMoS_2$ consists of several sidebands with a central peak shifted 176 ppm relative to a 1 M aqueous solution of CsCl.

Table 2. Measured NMR Parameters for $A_x(H_2O)_yMoS_2$

	$Li_x(H_2O)_yMoS_2$	$Na_x(H_2O)_yMoS_2$	$Cs_x(H_2O)_yMoS_2$
nucleus	^7Li	^{23}Na	^{133}Cs
δ(MAS)	-1.3	-3.4^b	176.3
$\Delta\omega$ (Hz)^a	586	2442	244

[a] Line width as obtained from the MAS NMR experiment. [b] Peak maximum.

The site anisotropy is also present in the ^{23}Na MAS spectrum of $Na_x(H_2O)_yMoS_2$. The central line in the spectrum (only second-order quadrupole effects can be observed here) has an asymmetric shape, indicating the asymmetry of the Na^+ position.

The static ^7Li NMR spectra measured at room temperature show satellites arising from first-order quadrupole perturbation. The intercalated Li^+ cations are obviously present in two different environments. The total width determined for one of the species is approximately 17.5 kHz. The shape broadening at the base might reflect a dynamic process or the inherent inhomogeneity of the material. The nature of a possible cation motion is difficult to characterize in the absence of variable-temperature measurements. Magic angle spinning of the same sample produced a narrow peak at -1.3 ppm. The chemical shift values observed in the cation NMR spectra of all the compounds confirm complete charge transfer from the intercalated species to the host lattice.

Discussion

The broad central peak which dominates the ^1H static spectra of the Li and Na intercalation compounds and which is also observed with lower amplitude in the static spectra of the Cs and K intercalates may be attributed to adsorbed water on the surface of the particles. Its intensity accounts for about 35% of the water content in the Li and Na samples. This signal, which is characteristic of unrestricted random motion of water molecules, is most probably the origin of the broad, intense peak in the ^1H MAS spectra of the Li, Na, and K intercalates. This suggests that these compounds contain two types of H_2O ligands, namely those which are directly coordinated to the intercalated A^+ cations and others which are adsorbed on the surface of the particles. This assumption is supported further by the change in the relative amplitudes of the central lines and the Pake doublet in the ^1H static spectra of $Na_x(H_2O)_yMoS_2$ upon evacuation. When the sample is exposed to moist air for a longer period of time, the original spectrum is restored.

A model was introduced previously to explain NMR data observed in the intermediate range of temperatures for hydrated groups 4 and 5 transition metal dichalcogenides of the type $A_x(H_2O)_yMS_2$.[3−8,16] It assumes an ordered anisotropic mobility of the water molecules in the intercalated phase. Since the measurements presented here were performed at ambient temperature, it is reasonable to expect that the results obtained for the chemical shifts and dipolar coupling constants can be interpreted in terms of this model. Comparison with the reported chemical shifts and dipolar interactions shows a reduction in the Pake doublet separation in the sequence Na, K, Cs which can be explained neither in terms of the structures of these phases nor on the basis of an increase in the H−H distance due to changes of the H−O−H bonding angle.[9,11−13]

An alternative explanation of this phenomenon is increased mobility of the water molecules in the sphere of the A^+ cations, leading to additional tilting motions around the C_2 axis. This may result in a reduced, direct dipolar interaction. A higher degree of freedom of water molecules in the $A_x(H_2O)_yMoS_2$ compounds (compared to the intercalation compounds of the elements in groups 4 and 5) may be due to structural distortions in the MoS_2 phases. Upon intercalation, the local coordination geometry of the Mo centers changes from trigonal prismatic to distorted octahedral, accompanied by the formation of different types of superstructures.[14,19] This affects the local structure of the A^+ cations as well as the mobility of diffusing water molecules.[16] The chemical shift anisotropy observed in the ^{133}Cs static NMR spectrum of $Cs_x(H_2O)_yMoS_2$ (Figure 5c) and the enhanced water mobility may be explained by such structural changes. The reduced dipolar splitting in the ^{1}H static NMR spectrum of the Cs intercalate (Figure 3a) indicates an arrangement of the H_2O molecules around the Cs^+ cation that differs from that shown in Figure 1a. Similar properties might be considered for the K intercalate.

The values found for the ^{1}H chemical shift anisotropies of $Na_x(H_2O)_yMoS_2$, $K_x(H_2O)_yMoS_2$, and $Cs_x(H_2O)_yMoS_2$ differ notably, despite the compounds having the same host lattice and degree of reduction. Ditchfield[21] calculated a value of −18.3 ppm for the chemical shift anisotropy of an isolated water molecule with axial symmetry around the O−H bonds. This corresponds to −9.5 ppm when the H−H vector is parallel to the hexagonal axis in the studied system. Only the chemical shift anisotropy of $Na_x(H_2O)_yMoS_2$ is close to the predicted value, while for the other two systems there is a small contribution with the opposite sign and axial symmetry around the hexagonal axis in the case of $Cs_x(H_2O)_yMoS_2$.

All studied compounds exhibit a weak and similar effective paramagnetic susceptibility at room temperature, consistent with the 2H → 1T phase transition (note that 2H-MoS_2 is diamagnetic, while 1T-MoS_2 shows Fermi paramagnetism). In agreement with magnetic susceptibility measurements, the isotropic chemical shifts in the ^{23}Na, ^{7}Li, and ^{133}Cs NMR spectra correspond to a complete charge transfer from the alkali metal to the host lattice.

$Li_x(H_2O)_yMoS_2$ is an exception from the observed trends in the static NMR experiments. This bilayered hydrated compound exhibits a proton spectrum characteristic of activated random motion, although the weak and unresolved wings can be tentatively attributed to intramolecular proton−proton dipole interactions. The corresponding ^{7}Li static spectrum shows the existence of two nonequivalent sites occupied by Li^+ cations. For $Li_x(H_2O)_yNbS_2$, quadrupole splitting in the wide-line NMR spectra was observed and interpreted as a change in the local coordination geometry of the Li^+ cations from octahedral to tetrahedral ($[Li(H_2O)_6]^+ \rightarrow [Li(H_2O)_4]^+$). However, coexistence of the octahedral and tetrahedral environments of the Li^+ cations was not detected; i.e., the Li^+ cations occupy different interstices in the van der Waals gap, depending on the temperature.[3−8] Although the dynamic behavior of $Li_x(H_2O)_yMoS_2$ was expected to be similar to that of $Li_x(H_2O)_yNbS_2$, there are certain differences. These can be attributed to the poor crystallinity and the distorted structure of this compound. Upon intercalation with Li^+ and subsequent hydration, the $a \times a$ structure of the host lattice changes to an $a \times 2a$ superstructure.[22,23] A similar superstructure was observed for the corresponding K compound. Whereas fully hydrated $K_x(H_2O)_yMoS_2$ has an $a \times a\sqrt{3}$ superstructure, an $a \times 2a$ superstructure can be observed at an early stage of the hydration reaction.[14,15,24] These structural changes are reflected by the water ligands of the intercalated Li^+ cations, which rearrange and may form two different environments. Both environments are connected by dynamic processes.

Conclusions

The dynamic behavior of the H_2O ligands in $A_x(H_2O)_yMoS_2$ (A = Li, Na, K, and Cs) intercalation compounds generally follow the trends observed for transition metal sulfide intercalates in groups 4 and 5 and is consistent with an ordered quasi two-dimensional mobility at room temperature. The reduced intramolecular dipole interaction observed in the present NMR experiments can be attributed to tilting motions of the H_2O molecules around their C_2 axes. This property is a consequence of the structural deviations and distortions of the $A_x(H_2O)_yMoS_2$ compounds with respect to 2H-MoS_2. The local environment of the alkali metal cations deviates considerably from a perfect octahedral arrangement, producing an effective field gradient at the cation site in the case of $Li_x(H_2O)_yMoS_2$, $Na_x(H_2O)_yMoS_2$, and $Cs_x(H_2O)_yMoS_2$. There seem to be two nonequivalent cation sites in the case of the Li intercalate. Both sites are occupied at room temperature.

Acknowledgment. V.A. thanks the Swiss National Science Foundation for providing financial support for this work (Grant 7BUPJ48572).

CM980780Z

---

[21] Ditchfield, R. *J. Chem. Phys.* **1976**, *65*, 3123.

[22] Qin, X. R.; Yang, D.; Frindt, R. F.; Irwin, J. C. *Phys. Rev. B* **1991**, *44*, 3490.

[23] Qin, X. R.; Yang, D.; Frindt, R. F.; Irwin, J. C. *Ultramicroscopy* **1992**, *42*, 630.

[24] Wypych, F.; Solenthaler, C.; Prins, R.; Weber, Th. *J. Solid State Chem.* **1999**, *144*, 430.